

First Steps to Future Applications of Spinal Neural Circuit Models in Neuroprostheses and Humanoid Robots

Yang Chen^{1,2}, Christian Bauer¹, Ole Burmeister¹, Rüdiger Rupp³,
Ralf Mikut¹

¹Forschungszentrum Karlsruhe GmbH, Institute for Applied Computer Science

²Universität Karlsruhe (TH)

³Orthopädische Universitätsklinik Heidelberg

E-Mail: {yang.chen, christian.bauer, ole.burmeister, ralf.mikut}@iai.fzk.de,
Ruediger.Rupp@ok.uni-heidelberg.de

1 Introduction

Modeling how humans control and coordinate their locomotion in daily life, such as walking and grasping, is an important research topic with promising application perspectives in medical and rehabilitation engineering, humanoid robotics, and other biological-inspired systems.

In recent years, the concept of central pattern generator (CPG), which has the ability to generate self-sustained rhythmic motor patterns even in the absence of supraspinal inputs and sensory afferent feedbacks [1, 2], has drawn much attention from engineers by showing novel application perspectives in neuroprostheses and humanoid robots.

Although for a thorough understanding of the CPG network there is still a long way to go, much work has been done in the last decades, ranging from deciphering the anatomical structure [3, 4] and computational modeling study [1, 5] to implementation of prototypes for engineering applications [6, 7].

In this paper, we outline the relevant topics of neural control for locomotion (Sec. 2), focusing on the functional significance of the CPG network in this context (Sec. 3). By employing a computational modeling approach (Sec. 4), we develop a simulation model (Sec. 5) and outline possible comparison strategies with human data (Sec. 6), aiming to gain further insights of spinal neural circuit models and evaluate their potentials in future neuroprosthetic and humanoid robotics applications.

2 Function and structure of motor control systems

The human neural control system for posture and movement is a complex, nonlinear system with a hierarchical structure (Fig. 1). At the top level, the volitional command is transmitted via the corticospinal tract, which directly connects the motor cortex to the spinal cord with cross over parts in the brainstem. The sensorimotor cortex is responsible for the strategic decision making, such as trajectory planning and grasp mode selection in dexterous grasping, as well as the high level sensory integration of visual and audio feedback. The cerebellum plays an important role in the precise coordination in time and space of locomotion. It is the processing center of the proprioceptive information (e.g. hip joint position) conveyed by the spinocerebellar tract [8, 9].

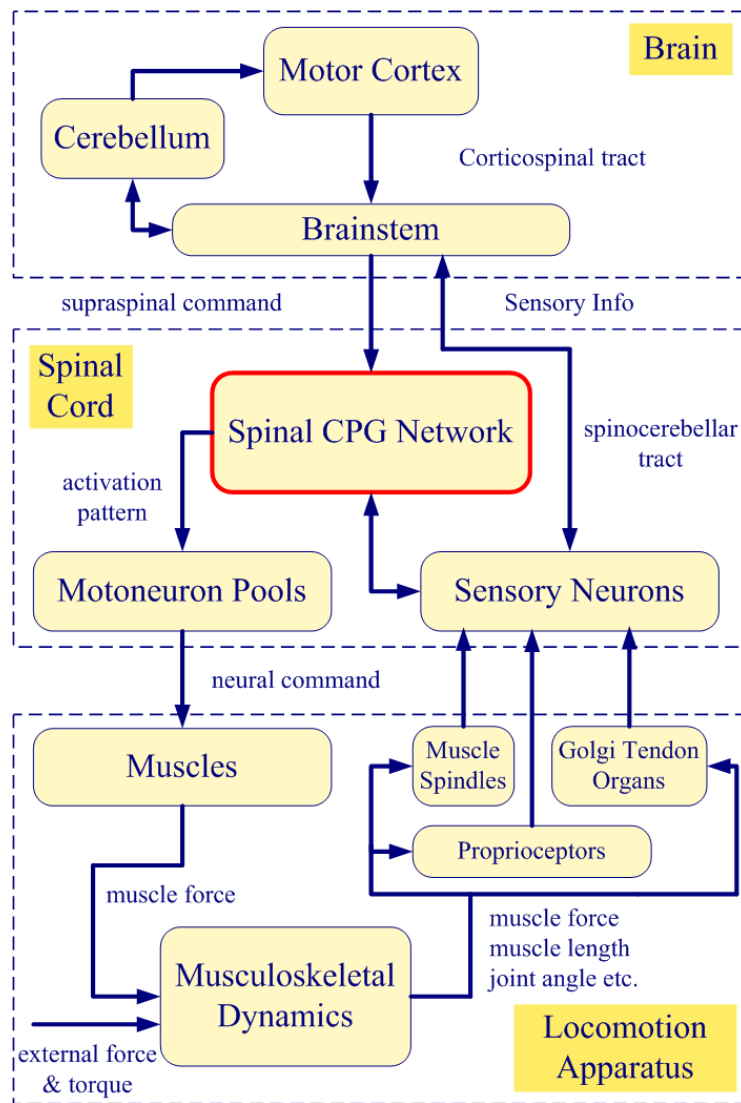


Figure 1: Block diagram of motor control system

The spinal cord forms the intermediate level and serves as coordinator and bridging element between the high level intelligence, the effectors and proprioceptors at the lower end of the system.

Opposing the traditional view, which believes that the neural reflexes only take up very primitive functions in a passive way, accumulating scientific evidences have proved that a significant level of control is mediated in the spinal cord and finally led to the concept of CPG.

Motoneurons in the ventral root of the spinal cord comprise the final common pathway of the neural commands. They interface with the musculoskeletal system via the neuromuscular junctions. The neuromuscular transformation, that is, how neural command is translated into muscle force, presents another modeling challenge to researchers. This process involves complex interactions between motoneurons and muscle fibers in the motor units, and the forward dynamics of the musculoskeletal system which converts the muscle force into movements of the locomotion apparatus. Unlike many common seen actuators in robots, biological muscles will actively adapt their stiffness with respect to

the muscle length measured by the muscle spindles and the force sensed by the golgi tendon organ.

A salient feature of the biological locomotor control system is the prevalence of bidirectional interaction at all levels. The CPG spinal circuit is by no means just an obedient servant who passively executes the commands sent by the motor cortex. Conversely, it actively shapes the supraspinal signal to integrate it into the context of ongoing locomotion. The biological evidence of this feature and its implication on robotic design is discussed in [10].

3 CPG network

3.1 Functional structure of the CPG network

The term CPG refers to a functional network consisting of a set of spinal neurons, which could generate rhythmic activation patterns resembling those observed in actual locomotion even in the absence of supraspinal controls. It is assumed that there is at least one such CPG for each limb. But opinions diverge as whether these CPGs are localized or distributed along the spinal cord of mammalian and primates including human [11]. The existence of such spinal reflex circuits are unequivocally proved in cats through the fictive locomotion observed in decerebrated unanesthetized preparations. Up till now a similar functional neural network in humans can only be demonstrated in an indirect way. However, sufficiently plenty of evidences have been obtained since recent years to make a convincing hypothesis of a spinal CPG network in human [12–14].

Deciphering the structure of the CPG network is traditionally carried out with help of electrophysiological analysis of the target species, and more recently with genetic methods [3]. In our work we take the model presented in [1, 5], which, despite its simple scheme, is able to intuitively outline the underlying neural structure of some properties observed in the fictive locomotion of cat. The involved neurons and their interconnection are depicted in Fig. 2.

Based on the half-center concept, the rhythmic pattern of the CPG network is generated by two populations of tightly coupled pace-maker neurons (RG-E and RG-F populations). The reciprocal inhibition mediated by the interneurons IN RG-E and IN RG-F between the two half-centers is responsible for the synchronized alternating transition between flexion and extension phases. In addition to the rhythm generation network, a pattern formation network consisting of the populations PF-E and PF-F, which are similar to those in the RG network but with a weaker bursting property, is incorporated here to allow a separate control of amplitude and timing of flexor and extensor motoneuron activities. This is independent of the frequency and phase of the locomotor oscillations set by the rhythm generation network. The output of the pattern formation network drives the collateral motoneuron pools to produce the motor activation patterns. The Renshaw cells, which are a set of interneurons providing recurrent inhibition to the motoneuron, form a local negative feedback loop to protect the muscle from over excitation, known as Renshaw inhibition.

Although the CPG network is able to produce rhythmic output independently, sensory inputs play an important role in sculpting the motor activation patterns. Observations in

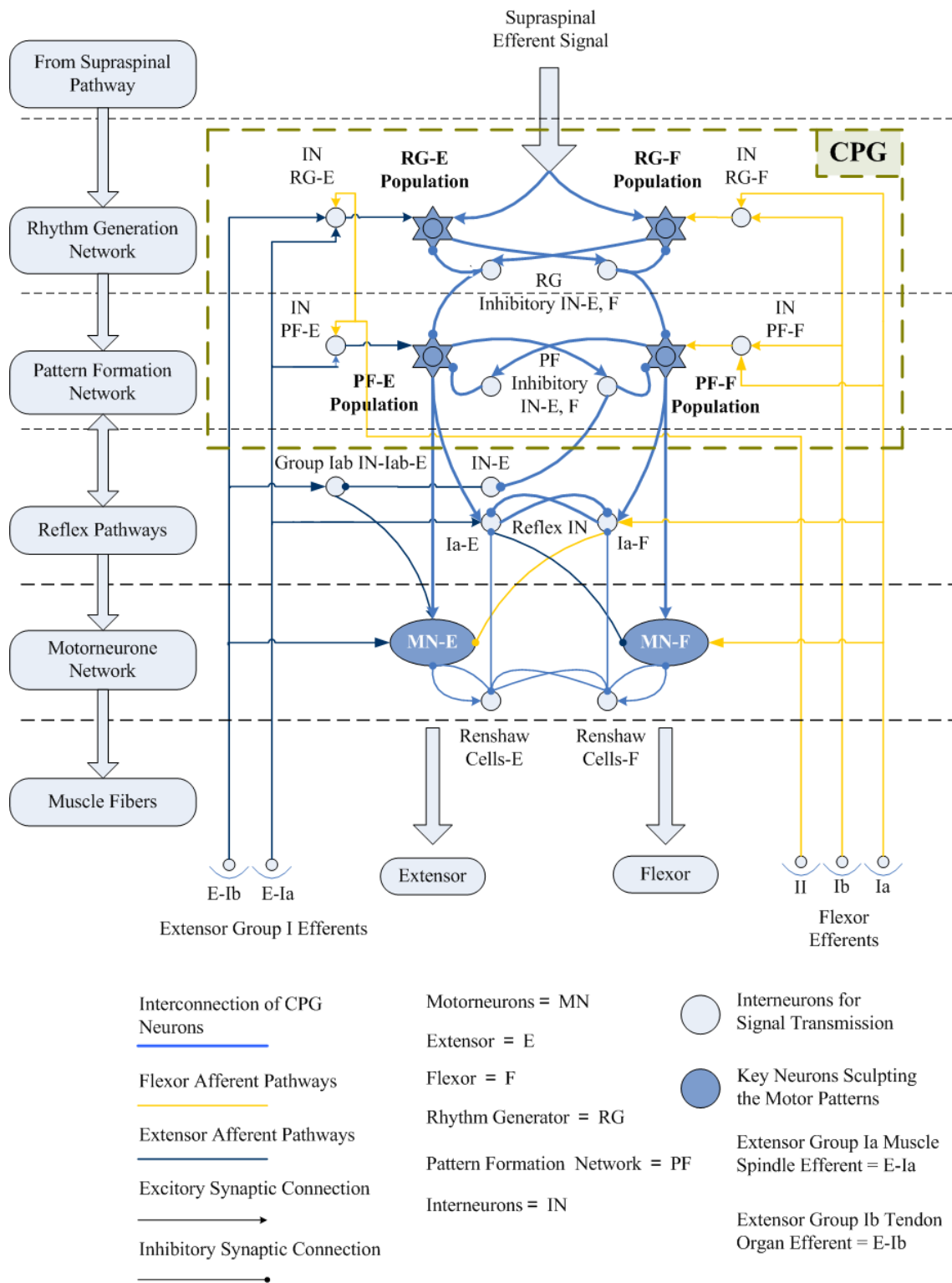


Figure 2: Structure of CPG network and the embedded reflex pathways [5, 15, 16]

healthy subjects and individuals with spinal cord injury (SCI) showed that load receptor inputs and hip joint afferents essentially contribute to the activation patterns of leg muscles during human locomotion [12, 16]. For a thorough review about the sensorimotor interaction in locomotion, see [15]. Some of the well understood reflex pathways are shown

in Fig. 2 to illustrate how the CPG and reflex circuits interact with each other to modulate the motoneuron activation pattern. The group I extensor afferents (Ia muscle spindles, Ib golgi tendon organ) contribute to the body-weight support during stance and control the stance-swing-transition by providing positive feedback loops in different levels of the network. These signals not only run through a disinaptic pathway via the interneuron IN-Iab-E, they are also fed to the CPG via the interneurons IN RG-E(F) and IN PF-E(F) for further processing. With this two level architecture of the CPG network, the group I extensor afferents can either control the proportion of extension phase via the PF network without changing the timing of the following cycles, or reset the locomotor rhythm by affecting the RG network, depending on the amplitude of stimulation. As suggested by the model in [5], the effect of Ia afferents on the RG network is weaker than their effect on the PF network. The flexor group I afferents have an analogue effect on the flexion phase, but the flexor group II is assumed to be excitatory to the extensor parts and hence forms a competing sensory signal to the flexor group I afferents. This could explain the spontaneous reversing reflex action of these afferents [5].

4 Mathematical models of single neurons

4.1 Model of pace-maker neurons

The Hodgkin-Huxley (HH) formalism enables a biophysically accurate mathematical description of single neurons. The general form of the single neuron model is given as follows:

$$C_m \cdot \frac{dV_m}{dt} = \sum_i^{n_{Ion}} I_{Ion,i} + \sum_i^{n_{Syn}} I_{Syn,i} + \sum_i^{n_{Ext}} I_{Ext,i} \quad (1)$$

where $C_m = 1\mu F/cm^2$ is the membrane capacity, and V_m the membrane potential.

Each external drive $I_{Ext,i}$ can be a constant current or a simple function like sine or ramp. The synaptic input I_{Syn} is the linear combination of all the event-triggered currents delivered by the connected n_{Syn} source neurons. The non-N-Methyl-D-Aspartic Acid (NMDA) glutamatergic synaptic current can be described as

$$I_{Syn,i} = \bar{g}_{Syn,i} \cdot w_i \cdot \exp\left(\frac{-t - t_{ls,i}}{\tau_{Syn,i}}\right) \cdot (V_m - E_{Syn,i}) \quad (2)$$

where $\bar{g}_{Syn,i} = 0.05mS/cm^2$ is the maximum conductance of synapses, w_i the connection weight, $t_{ls,i}$ is the last spike time of the i th neuron and $\tau_{Syn,i} = 5ms$ the time constant of the synaptic current. $E_{Syn,i}$, which is $-10V$ for excitatory synapses and $-40V$ for inhibitory synapses, is the reversal potential of synapses. For details of other more complicated models such as the alpha function form and the dual exponential form, see [2].

The characteristic behavior of a neuron is largely determined by the particular combination of ionic conductances $I_{Ion,i}$ found in its cell membrane and the interaction between them. When the basic Hodgkin-Huxley model is equipped with additional ion currents, which are linear superposition to the three ion channels of the classical model (sodium: I_{Na} , potassium: I_K , leakage: I_L), a much broader repertoire of behavior, such as the bursting property of pace-maker neurons in the CPG network, can be obtained. While the intrinsic mechanisms defining the rhythmogenic properties of CPG neurons remain

unknown, there is indirect evidence for the role of persistent sodium current I_{NaP} in rhythmogenesis [17, 18]. Together with the sodium, potassium, and leakage current in the original HH model, the ionic current in the pace-maker neuron consists of the following parts:

$$I_{Ion,Bursting} = I_{Na} + I_K + I_L + I_{NaP} \quad (3)$$

$$I_{Na} = g_{Na,max} \cdot m_{Na}^3 \cdot h_{Na} \cdot (V_m - E_{Na}) \quad (4)$$

$$I_K = g_{K,max} \cdot n_K^4 \cdot (V_m - E_K) \quad (5)$$

$$I_L = g_L(V_m - E_L) \quad (6)$$

$$I_{NaP} = g_{NaP,max} \cdot m_{NaP} \cdot h_{NaP} \cdot (V_m - E_{Na}) \quad (7)$$

where the constants E_x ($E_{Na} = 55mV$; $E_K = -85mV$; $E_L = -55mV$) are the reversal potentials of the ion currents, and g_x ($g_{Na} = 120mS/cm^2$; $g_K = 48mS/cm^2$; $g_{NaP} = 13mS/cm^2$; $g_L = 3mS/cm^2$) the maximum ionic conductances. The dynamics of the activation variables m_{Na} , n_K , m_{NaP} and inactivation variables h_{Na} , h_{NaP} all share a similar form derived from the original Hodgkin-Huxley formalism. Here the simplification is done by considering the fact that the activation variable m_{NaP} occurs on a much slower time scale than that of m_{Na} , so that the dynamics of (in-)activation variables represented generally by x is simplified to

$$\frac{dx}{dt} = \frac{x_\infty(V) - x}{\tau_x(V)}, x \in \{m_{Na}, h_{Na}, n_K, m_{NaP}, h_{NaP}\} \quad (8)$$

$$x_\infty(V) = \frac{1}{1 + \exp\left(\frac{V_m - \theta_x}{\sigma_x}\right)} \quad (9)$$

$$\tau_x(V) = \frac{\bar{\tau}_x}{\exp\left(\frac{V_m - \lambda_x}{\alpha_x}\right) + \exp\left(-\frac{V_m - \lambda_x}{\beta_x}\right)} \quad (10)$$

where $x_\infty(V)$ is the end value of the (in-)activation variables and $\tau_x(V)$ are the voltage dependent time constants. The other terms $\alpha_x, \beta_x, \lambda_x, \sigma_x, \bar{\tau}_x, \theta_x$ are constants selected to produce time curves of the ionic conductances similar to experimental observations, see [19].

In this model, the fast sodium current I_{Na} with its small time constant is in charge of the stiff rising edge of action potential, while the delayed-rectified potassium current I_K brings the membrane voltage back to the resting status shortly after the firing. The leakage current I_L , with g_L being a constant, is a static current accounting for the effect of other unspecified ion types. The maximum conductance of the persistent sodium channel $g_{NaP,max}$ set its weight on the total neuron behavior. If it remains under a certain threshold value, bursting and beating properties can no longer be obtained. The activation variable m_{NaP} works in a similar way to that of the fast sodium current. They are both responsible for the triggering of the action potential and the onset of the bursting activities. On the other hand, the inactivation h_{NaP} with its very large time constant $\tau_{h_{NaP}}(V)$ is in charge of the termination of the bursting pattern and thus determines the bursting period. By altering the leakage reversal potential E_L , typically from $-64mV$ to about $-50mV$, the neuron undergoes a transition from the quiescent state, through burster, to the beater status. Therefore, bursting is actually a gradual transitional state lying between these two ends and we can adjust the bursting ratio of the neuron by altering E_L . For a detailed discussion of the properties and interaction of the individual ionic currents, see [20].

4.2 Compartmental model of motoneurons

With help of experimental studies using ion channel blockers and neurotransmitters, complex firing patterns have been found in the vertebrate motoneurons. The bistable firing, which results from the interplay between several kinds of Ca^{2+} dependent currents, enables the motoneurons to convert short-lasting synaptic inputs into long-lasting motor output. Here we accept and use the model presented in [19].

The ion currents in soma include

$$I_{Ion,Moto,Soma} = I_{Na} + I_K + I_L + I_{CaN} + I_{K(Ca)} \quad (11)$$

$$I_{CaN} = g_{CaN,max} \cdot m_{CaN}^2 \cdot h_{CaN} \cdot (V_m - E_{Ca}) \quad (12)$$

$$I_{K(Ca)} = g_{K(Ca),max} \cdot m_{K(Ca)} \cdot (V_m - E_K) \quad (13)$$

$$g_{K(Ca),max} = \frac{Ca}{Ca + K_d} \quad (14)$$

$$\frac{dCa}{dt} = f(-\alpha \cdot I_{Ca} - k_{Ca} \cdot Ca) \quad (15)$$

and the dendrite is modeled with

$$I_{Ion,Moto,Dend} = I_{CaN} + I_{K(Ca)} + I_{CaL} \quad (16)$$

$$I_{CaL} = g_{CaL,max} \cdot m_{CaL} \cdot (V_m - E_{Ca}) \quad (17)$$

This two-compartment model was developed to reproduce some of the biophysical mechanisms underlying the Ca^{2+} -dependent regenerative responses observed in turtle spinal motoneurons under the injection of ion blockers. The constants g_L ($0.51mS/cm^2$), g_{CaL} ($0.33mS/cm^2$), g_{CaN} ($14mS/cm^2$ in soma, $0.3mS/cm^2$ in dendrite) and $g_{K(Ca),max}$ ($1.1mS/cm^2$ in soma, $5mS/cm^2$ in dendrite) are the newly added ion conductances of the L-like calcium conductance I_{CaL} , N-like calcium conductance I_{CaN} , and the calcium-dependent potassium current $I_{K(Ca)}$. Some of the parameters in Sec. 4.1 are changed correspondingly: $E_L = -65mV$, $g_K = 100mS/cm^2$, $g_L = 0.51mS/cm^2$. The activation and inactivation variables m_{CaN} , h_{CaN} , m_{CaL} follow the dynamics in accordance with the general form given in (8) to (10). The high threshold, inactivating current I_{CaN} allows calcium influx during action potentials and generates Ca^{2+} -based spikes in response to depolarizing current steps. The calcium-dependent potassium current $I_{K(Ca)}$ contributes to the slow after-hyperpolarization (AHP) following a spike. Its activation $m_{K(Ca)}$ is determined by the intracellular calcium concentration with (14), where $K_d = 0.2\mu M$ defines the half saturation level of this conductance. The intracellular calcium concentration Ca follows the dynamics in (15), where $f = 0.01$ describes the proportion of free Ca^{2+} , $\alpha = 0.0009mol \cdot \mu m/C$ converts the calcium current I_{Ca} into Ca^{2+} concentration and $k_{Ca} = 2ms^{-1}$ represents the Ca^{2+} removal rates.

4.3 Simplified model of spiking neurons

In order to overcome the prohibitive computational effort in large population simulations, the Hodgkin-Huxley type neural models can be reduced to a two-dimensional system of ordinary differential equations by using bifurcation methodologies. Izhikevich presented

a model which is mathematically elegant and yet retains some of the salient features of the biological realistic firing patterns in the form:

$$\frac{dv}{dt} = 0.04v^2 + 5v + 140 - u + I \quad (18)$$

$$\frac{du}{dt} = a(bv - u) \quad (19)$$

with a resetting paradigm of

$$\text{if } v \geq 30mV, \text{ then } \begin{cases} v = c \\ u = u + d \end{cases} \quad (20)$$

v and u are dimensionless variables representing the membrane potential and the membrane recovery rate originating from the activation of potassium current and inactivation of the sodium current in the Hodgkin-Huxley model. By varying the parameters a , b , c and d , a rich repertoire of firing patterns can be obtained with this model. The normal spiking state of interneurons corresponds to $a = 0.02$; $b = 0.2$; $c = -65$; $d = 2$; $I = 0$. For a detailed discussion on parametrization and the resulting firing behaviors, refer to [21].

5 Simulative evaluation

5.1 Modeling strategy for large-scale network simulation

The Hodgkin-Huxley model has the advantage of being able to replicate rich firing patterns as observed in the biological world and having a structure that can be directly derived from their biological counterparts, while the simplified model for spiking neurons is superior in terms of computational efficiency. To combine the strength of both approaches, we employ a hybrid model in our simulation. Since interneurons are only responsible for signal transmission, we use the Izhikevich model to describe them, so that a larger population with randomly distributed parameters and connection weights can be implemented. As to the pace-maker neurons and motoneurons, the HH model is utilized to produce a more biological realistic firing pattern.

5.2 Simulation results

We focus on the interaction of coupled pace-maker neurons in the CPG network and the resulting rhythmogenic properties of this topology. The low-level reflex circuits shown in Fig. 2 are not included at this stage. The model is implemented in software package NEURON [22]. Differential equations of the HH-style pace-maker neurons and motoneurons are solved using the *cnexp* method provided by NEURON. Other interneurons modeled with the simplified model for spiking neurons are solved with the *derivimplicit* method due to their nonlinear property.

The pace-maker neurons and motoneurons are modeled as concentrated elements to represent the corresponding neuron populations. Interneurons within the CPG network have a population of ten neurons. Heterogeneity is introduced by adding randomly distributed parameters for synaptic connection weights and delays. Simulation parameters are based on [1, 19, 21, 23] and adjusted to produce reasonable results.

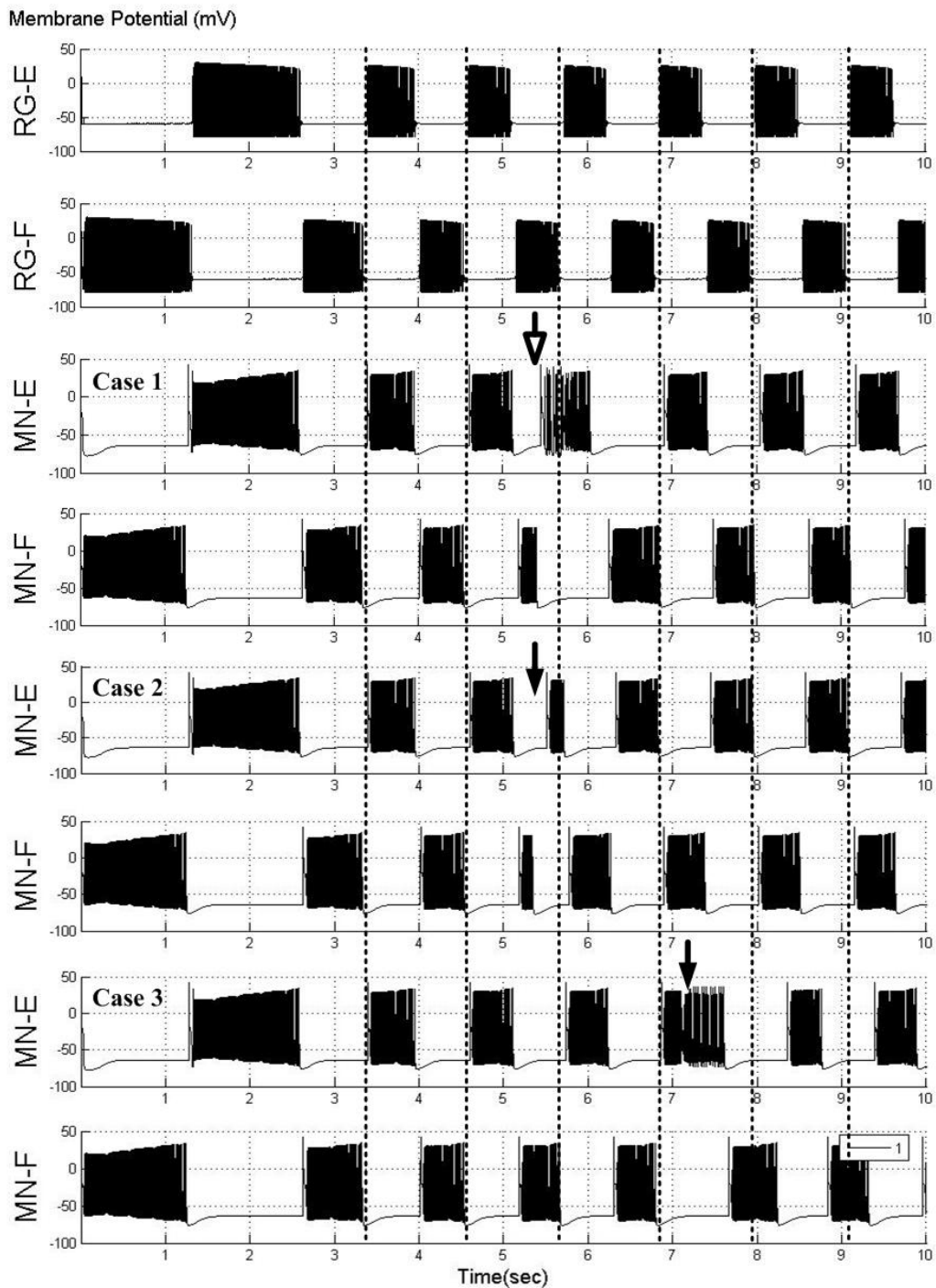


Figure 3: Modeling the effects of group Ia extensor afferent stimulation (see Fig. 2 for the different neuron types)

A short pulse with duration of 10ms is delivered to either side of the rhythm generation network to avoid the resonant state of the network resulting from a symmetrical initial state. The whole network is able to synchronize automatically without external inputs and finally settle down to the bursting frequency set by the rhythm generation neurons RG-E and RG-F. The alternating firing pattern of the flexor and extensor motoneurons

can represent the synergic movements of the corresponding muscles during stance and swing phase. The simulation result corresponds to a step cycle period of about 1.1s, see the output of pace-maker neurons in rhythm generation network (RG-E, RG-F) at top of Fig. 3.

To study how the rhythm generation network and the pattern formation network contribute to the sculpting of the output activation patterns under group Ia afferent inputs, we apply stimulations to different levels of the CPG with different timings. At the instants indicated by the arrows in Fig. 3, an afferent stimulus with a duration of 500ms is applied to the CPG. The hollow arrow indicates a stimulus to the PF-level via the interneuron PF-Ia-E, while solid arrows represent a strong stimulus influencing both the RG and PF levels. The output of the network in the extensor and flexor motoneurons MN-E and MN-F are shown in Fig. 3, aligned to the intrinsic rhythmic pattern set by the RG network. In Case 1, the Ia afferent causes a premature flexion without changing the timing of the following cycles. Conversely, a strong extensor Ia afferent can reset the locomotion rhythm by affecting the rhythm generation network via the sensory neuron RG-Ia-E. Notice the reversed phase in Case 2 after the external stimulation. On the other hand, Ia afferent can induce a prolongation of the extension phase, when the extensor motoneuron is activated (Case 3). This simulates the scenario that the transition from stance to swing phase can be delayed in prolonged steady load conditions. By this, the Ia afferent pathway and the CPG network actively contribute to the body-weight support during gait.

5.3 Discussion

This computational model of CPG network consisting of biological realistic neurons is able to generate coordinated rhythmic neural activation patterns through intrinsic mechanisms, and sculpts the outputs under the modulation of sensory information. We consider this model as a basis for subsequent modeling studies of reflex pathways and correlations between muscle activation patterns and locomotion movements.

A further development of this model is confronted with manifold challenges. The computational capacities of current simulation tools would soon reach their limit if network level behavior is under investigation (the current simulation needs about 30 min. to simulate 10 sec. of network behavior). Since this model is sensitive to subtle parameter changes and possess a high dimensional space of strong interrelated parameters, without analytical methods for the analysis of complex spiking neuron networks, application of optimization algorithms in parameter tuning would be a difficult issue.

6 Work in progress: modeling and evaluation of CPG structures

Future application perspectives of our model include: (1) as neural controller and locomotion pattern generator for bipedal-walking of humanoid robots; (2) as internal model for analysis of afferent and efferent modulations on human locomotion patterns; (3) based on the preceding item, as human-computer-interface in neuroprosthetic applications. One of the milestones on the way to the successful implementation of our model is the understanding of the synergetic interactions between the individual parts in the motor control system (Sec. 2). Or in other words, the linkage between motoneuron firing patterns and muscle contraction in rhythmic behaviors.

6.1 Software solutions

For the fulfillment of our research goal, we propose a simulation paradigm for closed-loop systems of locomotor control (Fig. 4). With respect to the simulation of biological realistic spiking neurons and their networks (see [24] for a comprehensive review), which serves as controller and coordinator in the whole system, software specialized for this application (e.g. NEURON) outperforms the general purpose simulation programs. They provide tailor-made numerical integration methods and prefabricated functions and classes describing various neural mechanisms and entities. SIMM is a commercially available software package for simulation and visualization of musculoskeletal models. MMS (Musculoskeletal Modeling in Simulink) [25] can translate the models developed in SIMM into Simulink blocks. The transformation from neural activation signal to muscle forces can be done by Virtual Muscle [26]. For visualization and analysis of neural spike trains and muscle EMG signals serves the Gait-CAD toolbox [27]. Human data can be incorporated into the closed loop system for parameter training and evaluation of simulation results. A related data set is discussed in the next section.

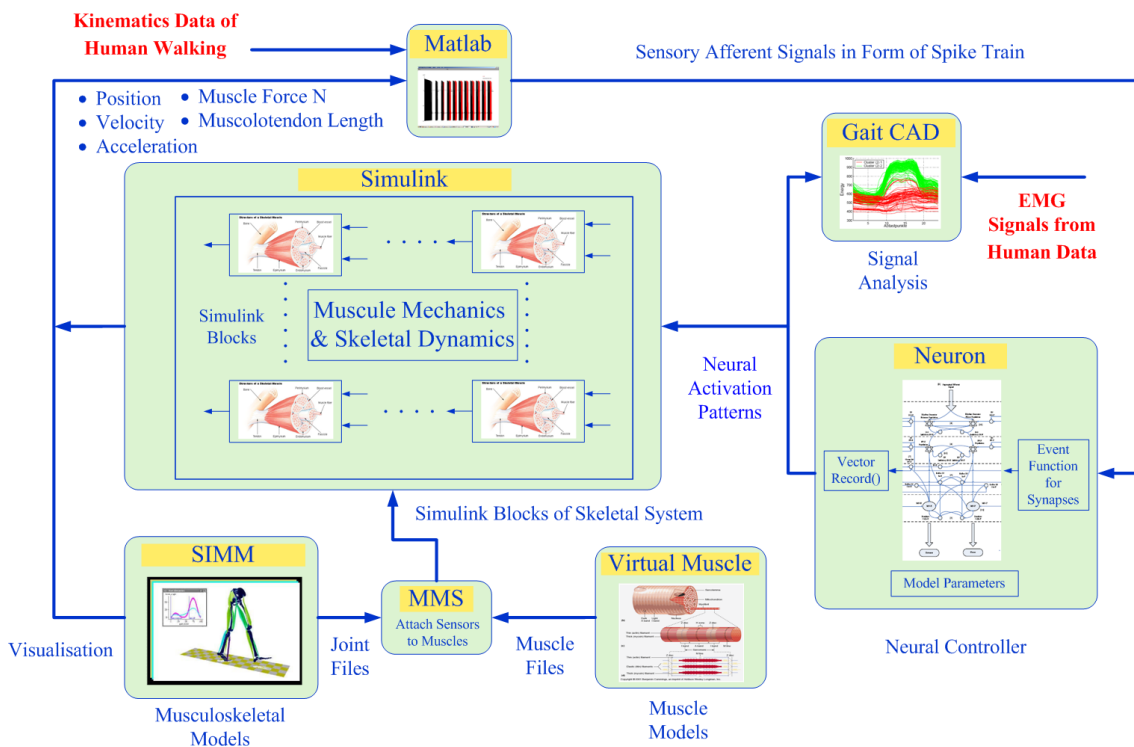


Figure 4: Possible simulation strategy for closed-loop systems of locomotor control

6.2 Human data

Data of human walking has been recorded from a 25-year-old female subject who walks on a treadmill with a speed of 1.1 m/s in the locomotion lab at the Orthopädische Universitätsklinik Heidelberg. Kinematic data which includes the joint angles of foot, knee, hip, pelvis, trunk, shoulder, and elbow in the sagittal, transversal and frontal planes is recorded with a commercially available 3D motion analysis system developed by Motion Analysis

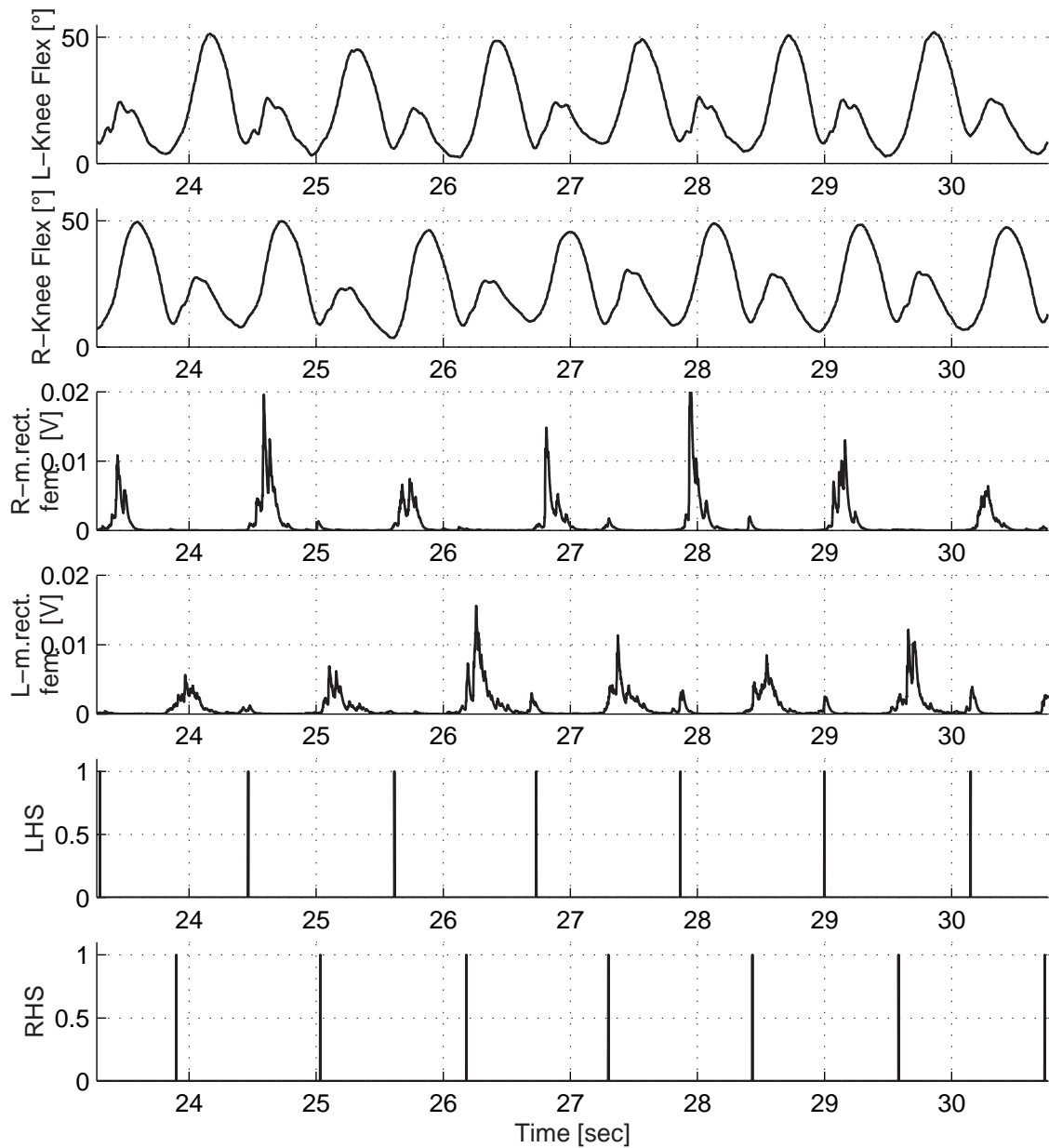


Figure 5: Examples of gait data: joint angles of the left and right knee in the sagittal plane, electromyographic signal of the left and right m. rectus femoris, and detected gait events for the left and right heel strike (top down)

Corp., USA with a sampling rate of 60 Hz. The hardware platform is described in [28]. In parallel to the kinematic data, EMG signals from the following muscles of both legs are recorded with a sampling rate of 960 Hz: m. gastrocnemius, m. tibialis anterior, m. biceps femoris, m. rectus femoris.

The following data preprocessing procedures are carried out:

- Gait events like heel strike (LHS, RHS) and toe off (LTO, RTO) at left and right side are detected.
- Joint angles are resampled at 960 Hz and low-pass filtered using a 1st order Infinite Input Response (IIR) filter with $a = 0.9$.
- Electromyographic signals are band-pass filtered using a 5th order Butterworth filter

with edge frequencies of 10 Hz and 350 Hz. The signals are further rectified and low-pass filtered by a 1st order IIR filter with $a = 0.95$.

Some selected results are presented in Fig. 5.

This human walking data provides information about gait events and triggering signals, which can be used to tune the parameters of the CPG network for the generation of more realistic muscle activation patterns. Furthermore, systematic analysis of differences between the recorded and the estimated muscle activations can be carried out using the methods from [29]. We also plan to obtain data of different walking speeds from the same subject and use them to analyze the influence of walking speed and temporal speed gradient on muscle activation patterns.

7 Conclusion

In this paper we gave an overview about the research done to identify the neurological structures which are responsible for the generation of rhythmic activation patterns for locomotion. Then the structure and components of these central pattern generators were elucidated and a simulation model, which has been implemented using NEURON, was introduced. This model will be used for further evaluations of human EMG data and locomotion, based on which it will be adapted for further uses in research for neuroprostheses and in the field of humanoid robotics.

Acknowledgements: This work has been performed within the framework of the German Humanoid Robotics Program (SFB 588) funded by the German Research Foundation (*DFG: Deutsche Forschungsgemeinschaft*). In particular, we would like to thank Christian Schuld for the preparation of the EMG data.

References

- [1] Rybak, I.; Shevtsova, N.; Lafreniere-Roula, M.; McCrea, D.: Modelling Spinal Circuitry Involved in Locomotor Pattern Generation: Insights from Deletions During Fictive Locomotion. *Journal of Physiology* (2006).
- [2] Bower, J.; Beeman, D.: *The Book of GENESIS*. Free Internet Edition. 2003.
- [3] Gordon, I.; Whelan, P.: Deciphering the Organization and Modulation of Spinal Locomotor Central Pattern Generators. *The Journal of Experimental Biology* 209 (2007), pp. 2007–2014.
- [4] Burke, R.; Degtyarenko, A.; Simon, E.: Patterns of Locomotor Drive to Motoneurons and Last-Order Interneurons: Clues to the Structure of the CPG. *Journal of Neurophysiology* 86(1) (2001), pp. 447–462.
- [5] Rybak, I.; Stecina, K.; Shevtsova, N.; McCrea, D.: Modelling Spinal Circuitry Involved in Locomotor Pattern Generation: Insights from the Effects of Afferent Stimulation. *Journal of Physiology* 577.2 (2006), pp. 641–658.
- [6] Ogihara, N.; Yamazaki, N.: Generation of Human Bipedal Locomotion by a Bio-Mimetic Neuro-Musculo-Skeletal Model. *Biological Cybernetics* 84 (2001), pp. 1 – 11.
- [7] Righetti, L.; Ijspeert, A.: Design methodologies for central pattern generators: an application to crawling humanoids. In: *Proceedings of Robotics: Science and Systems*, pp. 191–198. Philadelphia, USA. 2006.
- [8] Sherwood, L.: *Human Physiology: From Cells to Systems*. Thomson Books/Cole. 2004.
- [9] Schmidt, R.; Thews, G.; Lang, F.: *Physiologie des Menschen*. Berlin: Springer. 2000.
- [10] Cohen, A.; Boothe, D.: Sensorimotor Interactions During Locomotion: Principles Derived from Biological Systems. *Autonomous Robots* 7 (1999), pp. 239–245.

- [11] Ivanenko, Y.; Poppele, R.; Lacquaniti, F.: Spinal Cord Maps of Spatiotemporal Alpha-Motoneuron Activation in Humans Walking at Different Speeds. *Journal of Neurophysiology* 95 (2006), pp. 602–618.
- [12] Dietz, V.; Harkema, S. J.: Locomotor Activity in Spinal Cord-Injured Persons. *Application Physiology* 96 (2004), pp. 1954–1960.
- [13] Hultborn, H.; Nielsen, J.: Spinal Control of Locomotion - from Cat to Man. *Acta Physiology* 189 (2007), pp. 111–121.
- [14] Duysens, J.; de Crommert, H. W. A. A. V.: Neural Control of Locomotion; Part 1: The Central Pattern Generator from Cats to Humans. *Gait & Posture* 7(2) (1998), pp. 131–141.
- [15] Rossignol, S.; Dubuc, R.; Gossard, J.: Dynamic Sensorimotor Interactions in Locomotion. *Physiological Reviews* 86 (2006), pp. 89–154.
- [16] McCrea, D.: Spinal Circuitry of Sensorimotor Control of Locomotion. *Journal of Physiology* .
- [17] Crill, W.: Persistent Sodium Current in Mammalian Central Neurons. *Annual Reviews of Physiology* 58 (1996), pp. 349–362.
- [18] Del Negro, C.; Koshiya, N.; Butera, R.; Smith, J.: Persistent Sodium Current, Membrane Properties and Bursting Behavior of Pre-Boetzinger Complex Inspiratory Neurons in Vitro. *Journal of Physiology* 88 (2002), pp. 2242 – 2250.
- [19] Booth, V.; Rinzal, J.; Kiehn, O.: Compartmental Model of Vertebrate Motoneurons for Ca²⁺-Dependent Spiking and Plateau Potentials under Pharmacological Treatment. *Journal of Neurophysiology* 78 (1997), pp. 3371 – 3385.
- [20] Malmivuo, J.; Plonsey, R.: *Bioelectromagnetism - Principles and Applications of Bioelectric and Biomagnetic Fields*. Oxford University Press. 1995.
- [21] Izhikevich, E.: Simple Model of Spiking Neurons. *IEEE Transaction on Neural Networks* 14 (2003) 6, pp. 1569 – 1572.
- [22] Carnevale, N.; Hines, M.: *The NEURON Book*. Cambridge University Press. 2006.
- [23] Butera, R.; Rinzal, J.; Smith, J.: Models of Respiratory Rhythm Generation in Pre-Boetzinger Complex. I. Bursting Pacemaker Neurons. *Journal of Physiology* 82 (1999), pp. 382 – 397.
- [24] Brette, R.; Rudolph, M.; Carnevale, T.; Hines, M.; Beeman, D.; Bower, J.; Diesmann, M.; Goodman, P.; Harris, F.; Jr. Zirpe, M.; Natschlaeger, Pecevski, D.; Ermeuntrout, B.; Djurfeldt, M.; Lansner, A.; Rochel, O.; Vieville, T.; Muller, E.; Davison, A.; Boustani, S.; Destexhe, A.: Simulation of Networks of Spiking Neuron: A Review of Tools and Strategies. *Journal of Computational Neuroscience* in press (2007), pp. 1 – 66.
- [25] Davoodi, R.: *User's Guide to MMS: Musculoskeletal Modeling in Simulink*. Alfred E. Mann Institute, University of Southern California. 2002.
- [26] Cheng, E.; Brown, I.; Jerry, L.: *Virtual Muscle 3.1.5 User's Manual*. Alfred E. Mann Institute, University of Southern California. 2001.
- [27] Mikut, R.; Burmeister, O.; Reischl, M.; Loose, T.: Die MATLAB-Toolbox Gait-CAD. In: *Proc., 16. Workshop Computational Intelligence*, pp. 114–124. Universitätsverlag Karlsruhe. 2006.
- [28] Schablowski-Trautmann, M.: *Konzept zur Analyse der Lokomotion auf dem Laufband bei inkompletter Querschnittlähmung mit Verfahren der nichtlinearen Dynamik*. Ph.D. thesis, Universität Karlsruhe, Universitätsverlag Karlsruhe. 2006.
- [29] Wolf, S.; Loose, T.; Schablowski, M.; Döderlein, L.; Rupp, R.; Gerner, H. J.; Bretthauer, G.; Mikut, R.: Automated Feature Assessment in Instrumented Gait Analysis. *Gait & Posture* 23(3) (2006), pp. 331–338.